AGRICULTURE AND NATURAL RESOURCES

Journal homepage: http://anres.kasetsart.org

Research article

HMG-CoA reductase inhibitory activity of some selected *Citrus hystrix* constituents: *in silico* and *in vitro* evaluations

Suriphon Singha, Mayura Thongchuang, Yuttana Siriwattanasathien, Duangkamon Sangiamdee, Somyote Sutthivaiyakit*

Department of Chemistry and Center of Excellence for Innovation in Chemistry, Faculty of Science, Ramkhamhaeng University, Hua Mark, Bangkok 10240, Thailand.

Article Info

Article history:
Received 4 September 2025
Revised 10 October 2025
Accepted 25 October 2025
Available online 21 November 2025

Keywords:
Citrus hystrix DC.,
HMG-CoA reductase,
in silico Calculations,
in vitro Assay,
Rutaceae

Abstract

Importance of the work: Compounds with high mobility group A (HMGA) moiety from *Citrus hystrix* could be an effective HMG-CoA (an intermediate in the mevalonate and ketogenesis pathways) reductase inhibitor as statin drugs.

Objectives: To use *in silico* simulation and *in vitro* assay as tools to find HMG-CoA reductase inhibitor from *Citrus hystrix* constituents.

Materials and Methods: A set of 23 compound structures from *Citrus hystrix* was identified and optimized using the Gaussian 09 software at the B3LYP/6-31G(d) level of theory and subsequently docked into the protein structures of HMG-CoA reductase (https://www.rcsb.org/structure/1HW9) to find the best hit. The molecular dynamic simulation and *in vitro* assay were investigated.

Results: In total, 13 of the 23 compounds from *C. hystrix* had better molecular binding scores than simvastatin. Only three compounds—6′-*O*-(3″-hydroxy-3″-methylglutaryl)-6′,7′-dihydroxybergamottin (CH1), 6′,7′-dihydroxy-bergamottin and citrusoside G—that had high binding scores and were obtained in sufficient quantities—were chosen for further molecular dynamic simulation and *in vitro* HMG-CoA reductase inhibition assay. CH1 had better binding affinity than simvastatin, with both these having slightly different types and numbers of binding interactions. In the *in vitro* evaluation, CH1 had the strongest activity. However, the three compounds were less active than simvastatin. The discrepancy between the *in vitro* evaluation and *in silico* results may have been due partly to the limited solubility of the hydrophobic compounds in the test buffer solution used.

Main finding: Evidence was provided that CH1 in *C. hystrix* was a promising HMG-CoA reductase inhibitor and this plant may be a useful functional food plant candidate for the treatment and alleviation of hyperglycemia and Alzheimer disease.

* Corresponding author.
E-mail address: somyote_s@yahoo.com (S. Sutthivaiyakit)

https://doi.org/10.34044/j.anres.2025.59.6.13

Introduction

Hyperlipidemia is the medical term for high levels of lipids, particularly cholesterol and triglycerides, in the blood (Jameson, et al., 2022). These fats are essential for normal body function; however, when their levels are too high, they can cause a build up of fatty deposits, known as plaque, on the body's blood vessel walls, thus increasing the risk of cardiovascular diseases such as heart attack, stroke and atherosclerosis (National Health Service, UK, 2022a). The causes of hyperlipidemia can be genetics, poor diet, lack of exercise, obesity, diabetes, smoking, alcohol overuse and certain medications (National Heart, Lung and Blood Institute, 2024). Treatment of hyperlipidemia can involve a changed lifestyle, regular monitoring and use of proper medications (Jameson, et al., 2022). Statins are a class of medication that can lower cholesterol levels and reduce the risk of heart disease and stroke (Stein, 2002). Statins function by binding to the active site of HMG-CoA (an intermediate in the mevalonate and ketogenesis pathways) reductase (HMGCR) and thus inhibiting the enzyme and consequently reducing cholesterol production in the liver (Istvan et al., 2000; Istvan and Deisenhofer, 2000 and 2001; Igel et al., 2001; Istvan, 2003). However, statins can cause side effects, such as muscle pain or weakness, elevation of liver enzymes, increased blood sugar causing a risk of Type 2 diabetes and, in rare cases, serious muscle breakdown (National Health Service, UK, 2022b).

With the belief that certain natural products may be effective in treating hyperlipidemia with a lower risk of negative side effects, attention has been directed to alternative medicines of plant origin. For example, several plant extracts have been investigated *in vitro* against HMG-CoA reductase and some extracts have produced rather high half maximal inhibitory concentration (IC_{50}) values; however, no pure compounds were tested in those reports (Jung et al., 2005; Gholamhoseinian et al., 2010; Baskaran et al., 2015). Recently, several *in silico* approaches for the screening of HMG-CoA reductase inhibitors were documented and helped to identify some best-hit compound structures (Junaidin et al., 2022; Mazumder et al., 2024; Dagar et al., 2025).

Citrus hystrix DC (Rutaceae) is known in Thailand as "makrut", where its leaves and fruits are commonly used in Thai cooking recipes (Buathong and Duangsrisai, 2023). Its phytochemicals and uses were recently reviewed (Siti et al., 2022; Zhao et al., 2023). Phytochemical investigations have revealed that this plant contains diverse types of secondary metabolites, including prenylfuranocoumarin–hydroxymethylglutaric acid (high mobility group A, HMGA) conjugates (Youkwan et al., 2010; Seeka et al., 2016). The current study investigated whether the HMGA moiety present in some of the isolates could bind competitively to the HMG-CoA reductase active sites, which can lead to the suppression of mevalonate generation, thus resulting in a decrease in cholesterol formation. Two 3-hydroxymethylglutaryl flavonoid glycosides (brutieridin and melitidin) were isolated from *Citrus bergamia* Risso, with computations of the binding energy in a protein-like medium indicating that both compounds seemed to be good candidate competitive inhibitors of HMG-CoA reductase with respect to the binding of HMG-CoA (Di Donna et al., 2009; Leopoldini et al., 2010). Based on this information, molecular docking simulations were carried out for 23 structures of the prenylfuranocoumarin–hydroxymethylglutaric acid (HMGA) conjugates and related isolated compounds (Youkwan et al., 2010; Seeka et al., 2016). The current study investigated the best-hit compounds further using molecular dynamic simulations as well as *in vitro* HMG-CoA reductase inhibitory activity.

Materials and Methods

System information

Computational simulations and visualizations were performed using an Intel® Xeon® E5-2680 V3 dual core CPU 2.50 GHz processor (Intel Corp.; Santa Clara, CA, USA), with the Windows 11 Pro operating system (Microsoft Corp.; Redmond, WA, USA) and the Ubuntu 22.04.1 LTS, 64-bit open source software operating system (Canonical; London, UK). The software utilized in this study consisted of Gaussian 09 (Frisch et al., 2010), AutoDock 4.2 (Morris et al., 1998), AutoDock Tools (ADT) V. 1.5.6 (Morris et al., 2009), AutoDock Vina V. 1.1.2 (Trott and Olson, 2009) and BIOVIA Discovery Studio Visualizer V. 21.1 software (BIOVIA, 2020). The Molecular Dynamics (MD) simulations of the protein-ligand complex were performed using Desmond V. 6.5 (Schrödinger, 2021) to evaluate the structural stability over time.

The current study investigated a set of 23 compound structures of *Citrus hystrix* (Youkwan et al., 2010; Seeka et al., 2016). Candidate compound structures were optimized using Gaussian 09 at the B3LYP/6-31G(d) level of theory and subsequently docked into the protein structures of HMG-CoA reductase (PDB: 1HW9, 2.33 Å; Istvan et al., 2000 and 2001;

Igel et al., 2001; Junaidin et al., 2022), obtained from the Protein Data Bank (https://www.rcsb.org/structure/1HW9). Both the protein and ligand structures (23 compounds) were prepared for docking using AutoDock Tools (Morris et al., 2009). The protein structure was prepared by removing water molecules, adding polar hydrogens, merging nonpolar hydrogens and lone pairs, and assigning Kollman charges. Ligands were assigned Gasteiger partial charges, with torsions kept at default settings. A grid box size of 95 Å × 95 Å × 95 Å was centered on the crystallographic coordinates of simvastatin in the binding pocket (center: x = 3.928, y = –9.204, z = –11.325). Molecular docking simulations were performed using AutoDock Vina and the resulting docking poses were visualized and analyzed using BIOVIA Discovery Studio Visualizer (see Tables 1 and S1).

Table 1 Molecular docking interactions between HMG-CoA—reductase (HMGCR)/simvastatin and HMGCR/selected isolated compounds

Compound	Residues	Interaction	Distance (Å)	Docking score (kcal/mol)
Simvastatin	LYS735*	Hydrogen Bond	1.81	–7.4
	ARG590*	Hydrogen Bond	1.80	
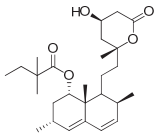	LYS691*	Hydrogen Bond	1.88	
	ASP690*	Hydrogen Bond	2.09, 1.81	
	ALA751	Hydrogen Bond	1.92	
	CYS561	Alkyl	5.03, 3.66	
	LEU853	Alkyl	5.11	
	LEU562	Alkyl	4.37	
	HIS752	Pi-Alkyl	4.68	
6′-*O*-(3″-Hydroxy-3″-methylglutaryl)-6′,7′-dihydroxybergamottin (CH1)	LYS735*	Hydrogen Bond	1.91	–9.3
	ARG590*	Hydrogen Bond	2.46	
	MET655	Hydrogen Bond	3.02	
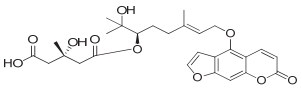	GLY656	Hydrogen Bond	2.06	
	LYS691*	Hydrogen Bond	2.14	
	LYS692	Hydrogen Bond	2.74, 2.68	
	SER684	Hydrogen Bond	3.01	
	ASN658	Hydrogen Bond	1.95	
	ASP690*	Hydrogen Bond	1.44	
	ASP767	Pi-Anion	4.74	
	GLY808	Pi-Donor Hydrogen Bond	2.62	
	MET655	Pi-Sigma	2.88	
	MET655	Pi-Alkyl	4.82	
Citrusoside G	ASN567	Hydrogen Bond	2.16	–9.4
	ASN755	Hydrogen Bond	2.76	
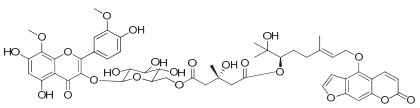	ARG590*	Hydrogen Bond	2.92, 2.27, 2.00	
	LYS691*	Hydrogen Bond	2.07	
	GLU665	Hydrogen Bond	1.48	
	ASP690*	Hydrogen Bond	1.95, 1.93	
	GLU559	Hydrogen Bond	2.15	
	ALA564	Alkyl	4.60, 3.86	
	ARG568	Alkyl	5.34	
	ALA856	Alkyl	3.23	
	CYS561	Alkyl	3.74	
	ALA564	Pi-Alkyl	4.71	
	ARG568	Pi-Alkyl	4.47, 4.01	
	ARG571	Pi-Alkyl	5.10	
	VAL720	Pi-Alkyl	5.46	
	MET657	Pi-Alkyl	5.12	
6′,7′-Dihydroxybergamottin	LYS735*	Hydrogen Bond	2.08	–7.6
	ALA525	Hydrogen Bond	2.92, 2.06	
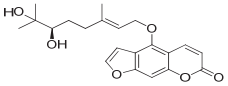	ARG590	Pi-Cation	4.10, 3.74, 3.23	
	LEU853	Pi-Alkyl	4.99	

* = commonly found active residues among these compounds (see also Istvan et al., 2000).

Validation of docking

The molecular docking procedure was performed by redocking simvastatin into the active site of HMG-CoA reductase (1HW9) to determine the appropriate binding parameters for the docking of AutoDock Vina. The accuracy of the redocking was evaluated by calculating the root mean square deviation (RMSD) between the redocked ligand and the X-ray crystallographic assembly of simvastatin. An RMSD value of the co-crystallized ligand of less than 2.0 Å (Fig. 1) indicated that the docking method used was sufficiently accurate in the prediction of the binding mode of the ligand (Silva et al., 2021; Mazumder et al., 2024).

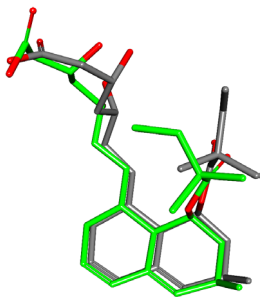

Fig. 1 Redocking validation of co-crystallized ligand, where crystal structure of simvastatin (green) is superimposed with redocked pose (gray)

Molecular dynamics

Molecular dynamic (MD) simulations were performed to inspect the best variability and conformational variations of different binding modes of ligand-protein complexes using the previously published protocol and references cited (Mazumder et al., 2024). The protein-ligand complexes were prepared using the Desmond system builder and solved using the pre-defined SPC solvent model. Orthorhombic boundary conditions were applied to the simulation box, maintaining a 10 Å buffer between the solute and the box edges. The system was neutralized with appropriate counter ions (Na^+/Cl^-). The MD simulations were carried out under the NPT ensemble at 300 K and 1.01325 bar for 100 ns, with trajectory data recorded every 100 ps for subsequent structural and interaction analyses. Interaction diagrams were generated using the Desmond module to examine the simulation results.

Chemical and reagents for in vitro analysis

The HMG-CoA reductase enzyme and relevant reagents were obtained as an assay kit from Sigma-Aldrich (St. Louis, MO, USA) and DMSO ReagentPlus® was obtained from Sigma-Aldrich (Saint-Quentin-Fallavier, France).

HMG-CoA reductase assay

HMGCR inhibitory activity evaluation was based on the protocol reported by Iqbal et al. (2014) Baskaran et al. (2015) and Zaborowska et al. (2022) using the HMGCR assay kit. Simvastatin was used as the standard drug. The inhibition of the HMGCR assay was based on the consumption of nicotinamide adenine dinucleotide phosphate (NADPH) in the presence of the substrate HMG-CoA, which was monitored by the decrement of the absorbance at 340 nm. In brief, to examine the inhibition of selected isolates on HMGCR activity, each well of a 96-well plate contained 1 µL of at least five serial concentrations of the samples (0.4–80 mg/mL to obtain final concentrations of 2–400 µg/mL) dissolved in dimethyl sulfoxide (DMSO), 4 µL of NADPH (to obtain a final concentration of 400 µM) and 12 µL of HMG-CoA (to obtain a final concentration of 400 µM) in a final volume of 0.2 mL of 100 mM potassium phosphate buffer, pH 7.4, containing 120 mM potassium chloride (KCl), 1 mM ethylenediaminetetraacetic acid and 5 mM dithiothreitol. The enzymatic reaction was initiated by the addition of 2 µL of the catalytic domain of human recombinant HMGCR. Simvastatin within a concentration range of 5–100 µg/mL (to obtain final concentrations of 25–500 ng/mL) was used as the standard drug, while a sample-free DMSO served as the control. A final concentration of 0.5% DMSO was established in each well plate.

The rates of reaction were investigated at 37°C. The decrease in absorbance of NADPH was recorded every 20 s for up to 10 min at 340 nm using a microplate spectrophotometer (Multiskan™ SkyHigh; Thermo Scientific; Waltham, MA, USA).

The enzyme activities were determined in the unit of specific activity (Units/mgP) defined as the units of micro moles of NADPH oxidized per minute per milligram of protein using Equation 1, as provided by the manufacturer (Sigma-Aldrich St. Louis, MO, USA):

$$\text{Units/mgP} = [\Delta A_{340}/\text{min sample} - \Delta A_{340}/\text{min blank}) / 12.44 \times 0.002 \times 0.6 \times 0.55] \times 0.2 \quad (1)$$

where ΔA_{340}/min is the absorbance difference between the two time points in the linear range at least 2 min apart, sample is the reaction with HMGCR and blank is to the reaction without HMGCR, 0.2 mL is the total volume of the reaction, 12.44 L/(mmol·cm) is derived from the 2 M of NADPH consumed in the reaction (since the extinction coefficient for NADPH at

340 nm is 6.22 L/(mmol·cm), 0.002 mL is the volume of the enzyme used in the assay, 0.6 mgP/mL is the enzyme concentration; and 0.55 cm is the value of the light path for the plates.

The results of the sample inhibition were presented in terms of the percentage inhibition compared to that of the control when the NADPH oxidation reaction occurred for a sample-free DMSO. The percentage of HMGCR inhibition was calculated using Eq. 2:

$$\% \text{ Inhibition} = \frac{\text{Units/mgP}_{control} - \text{Units/mgP}_{sample}}{\text{Units/mgP}_{control}} \times 100 \quad (2)$$

where the Units/mgP control is the unit of specific activity of the control when the HMGCR reaction with a sample-free DMSO while sample is the HMGCR reaction with a test substance.

The half-maximal inhibitory concentration (IC_{50}) value, representing the concentration at which 50% inhibition is achieved, was determined by analyzing the relationship between the percentage of HMGCR inhibitory activity and the sample concentration. All experiments were performed in triplicate.

Results and Discussion

Validation of the molecular docking calculations, based on the RMSD value of the co-ligand of 1HW9 of 1.16 Å (Fig. 1), indicated that the constructed docking method was sufficiently accurate in predicting the binding mode of the ligand, as it was less than 2.0 Å (Silva et al., 2021; Mazumder et al., 2024).

The molecular docking calculations of the 23 compound structures of the previously isolated compounds from the *Citrus hystrix* peels with 1HW9 protein revealed that 13 of these compounds had docking scores in the range –12.2 kcal/mol to –7.4 kcal/mol, while the standard drugs (pravastatin and simvastatin) had docking scores of –6.9 and –7.4 kcal/mol, respectively (Table S1). Among the 13 compounds, only 3 [6′-*O*-(3′′-hydroxy-3′′-methylglutaryl)-6′,7′-dihydroxybergamottin (CH1), 6′,7′-dihydroxy-bergamottin and citrusoside G] were considered for further MD simulation and *in vitro* study, based on their high docking scores and their ready availability. The computational results, consisting of binding residues, types of interactions, distances and docking scores, are shown in Fig. 2 and Table 1.

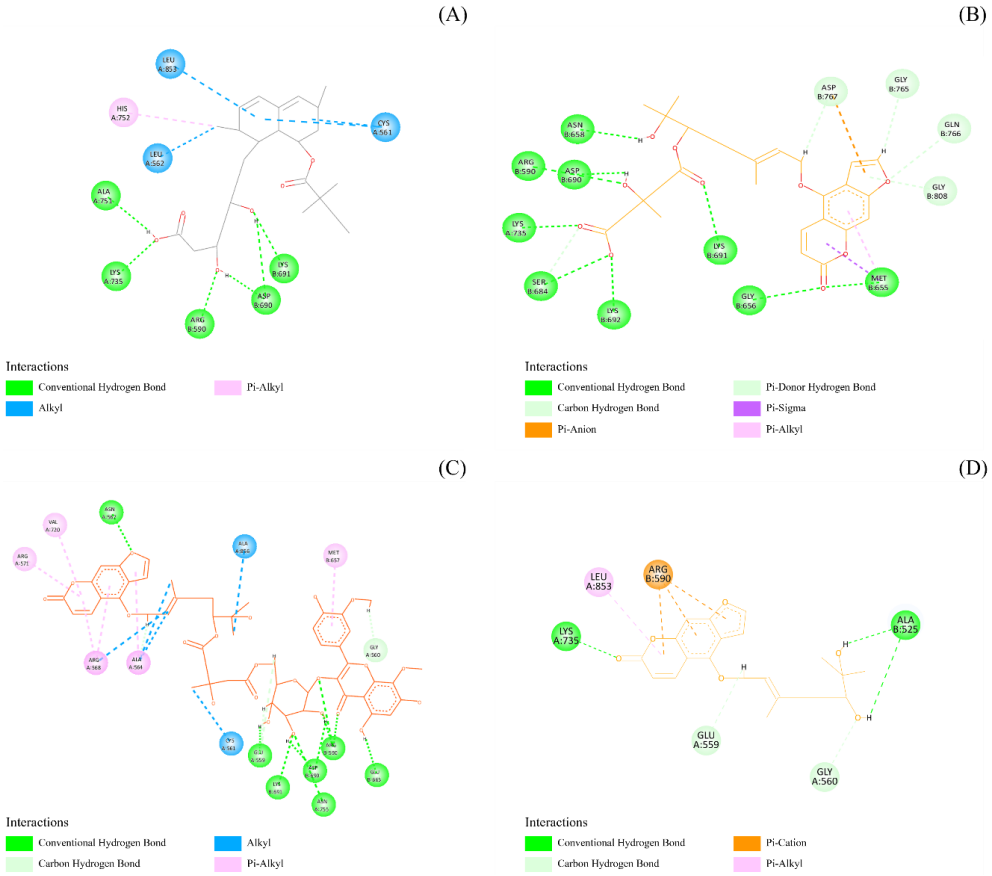

Fig. 2 Molecular docking interactions between 1HW9 and inhibitors: (A) simvastatin; (B) 6′-*O*-(3′′-hydroxy-3′′-methylglutaryl)-6′,7′-dihydroxybergamottin (CH1); (C) citrusoside G; (D) 6′,7′-dihydroxybergamottin (illustrations obtained using BIOVIA Discovery Studio software).

Based on the molecular docking calculations, the selected three compounds had better binding scores than simvastatin, with all four compounds having different types and numbers of binding interactions, as shown in Table 1 and Fig. 2. CH1 had the highest hydrogen bonding interactions.

Since the docking scores for CH1 and citrusoside G were similar, additional criteria were used concerning the physicochemical properties prediction of simvastatin and the three isolates (Table 2), obtained from SwissADME (www.swissadme.ch). These additional criteria helped to decide which compound should be chosen for further MD simulation. Based on the *in silico* ADME prediction, the physicochemical property of CH1 was more acceptable than citrusoside G (Table 2) (Daina et al., 2014 and 2017; Daina and Zoete, 2016).

To understand the protein-ligand complex dynamic behavior and stability, MD simulations were undertaken for apo-protein and the protein-ligand complexes of 1HW9-simvastatin and 1HW9-CH1 over a 100 ns time scale. In the 1HW9-simvastatin and 1HW9-CH1 complexes, the protein-ligand complex RMSD values of the proteins of both complexes were more or less similar to the apo-protein (Fig. 3). The RMSD values of the ligands in both complexes remained rather stable until 100 ns. The highest RMSD values of both proteins in both protein-ligand complexes were around 2.0 Å, indicating that both complexes were equally stable with no conformational changes. The strengths of the interaction between the protein-simvastatin and protein-CH1 complexes were obtained based on the calculation of the MM/GBSA binding energy values (–34.637 and –52.874 kcal/mol, respectively). Based on these calculations, CH1 had better binding affinity than simvastatin.

The root mean square fluctuation (RMSF) is useful for characterizing local changes along the protein chain, including protein flexibility. In this plot, the peaks indicate areas of the protein that fluctuate the most during the simulation. It is common to observe that the tails (N- and C-terminals) fluctuate more than any other part of the protein. Usually, secondary structure elements, such as α-helices and β-strands, are more rigid than the unstructured part of the protein and thus fluctuate less than the loop regions (Shehu and Kavraki, 2012). Based on the calculations (Fig. 4), the 1HW9-CH1 complex had comparable rigidity to the 1HW9-simvastatin complex; however, the 1HW9-CH1 complex had a slightly higher residue index, indicating more interactions between CH1 and protein residues.

Table 2 Physicochemical properties of simvastatin, CH1, citrusoside G and 6′,7′-dihydroxybergamottin (using SwissADME)

Parameters	Simvastatin	CH1	Citrusoside G	6′,7′-Dihydroxybergamottin
Physicochemical properties				
Formula	$C_{25}H_{40}O_6$	$C_{27}H_{32}O_{10}$	$C_{50}H_{54}O_{22}$	$C_{21}H_{24}O_6$
Molecular weight	436.58 g/mol	516.54 g/mol	1006.95 g/mol	372.41 g/mol
Heavy atoms	31	37	72	27
Aromatic heavy atoms	0	13	29	13
Fraction Csp3	0.76	0.44	0.40	0.38
Rotatable bonds	11	13	21	7
H-bond acceptors	6	10	22	6
H-bond donors	3	3	8	2
Molar refractivity	122.23	135.84	253.19	103.90
TPSA	104.06 Å²	156.64 Å²	334.15 Å²	93.04 Å²
Lipophilicity				
Log $P_{o/w}$ (iLOGP)	3.66	3.85	5.24	3.56
Water Solubility				
Log *S* (ESOL)	-4.64	-4.06	-7.40	-3.93
Solubility class	Moderately soluble	Moderately soluble	Poorly soluble	Soluble
Pharmacokinetics				
Gastrointestinal absorption	High	Low	Low	High
BBB permeant	No	No	No	No
Druglikeness				
Violation of Lipinski's rule	0	1	3	0
Violation of Ghose rule	1	2	3	Yes
Violation of Veber rule	1	2	2	Yes
Bioavailability score	0.56	0.11	0.17	0.55

Fraction Csp3 = fraction of carbon insp3 hybridization; TPSA = topological polar surface area;
Log $P_{o/w}$ = *n*-octanol/water partition coefficient; iLOGP = implicit log *P* method; Log *S* = logarithm of solubility; ESOL = estimated solubility, BBB = blood brain, barrier penetration.

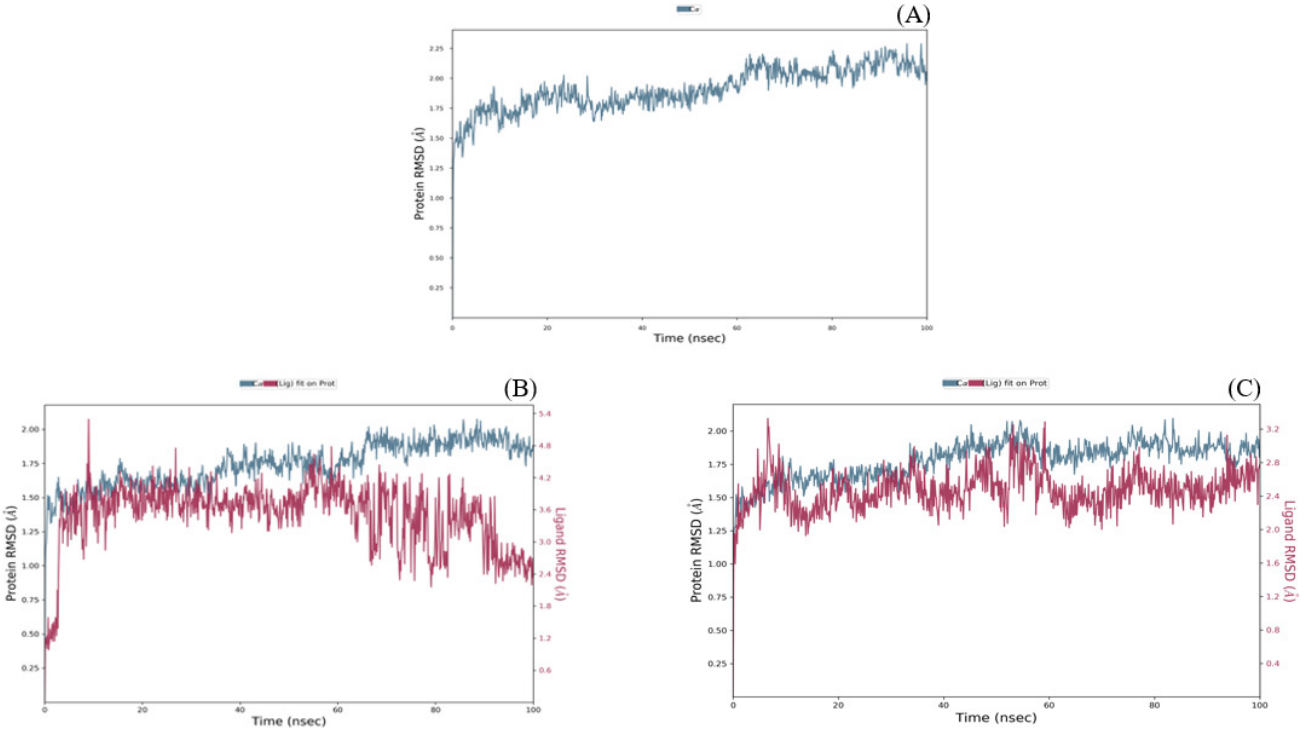

Fig. 3 Root mean square deviation plots of: (A) apo-protein 1HW9; (B) 1HW9-simvastatin complex; (C) 1HW9–6′-*O*-(3″-hydroxy-3″-methylglutaryl)-6′,7′-dihydroxybergamottin (CH1) complex

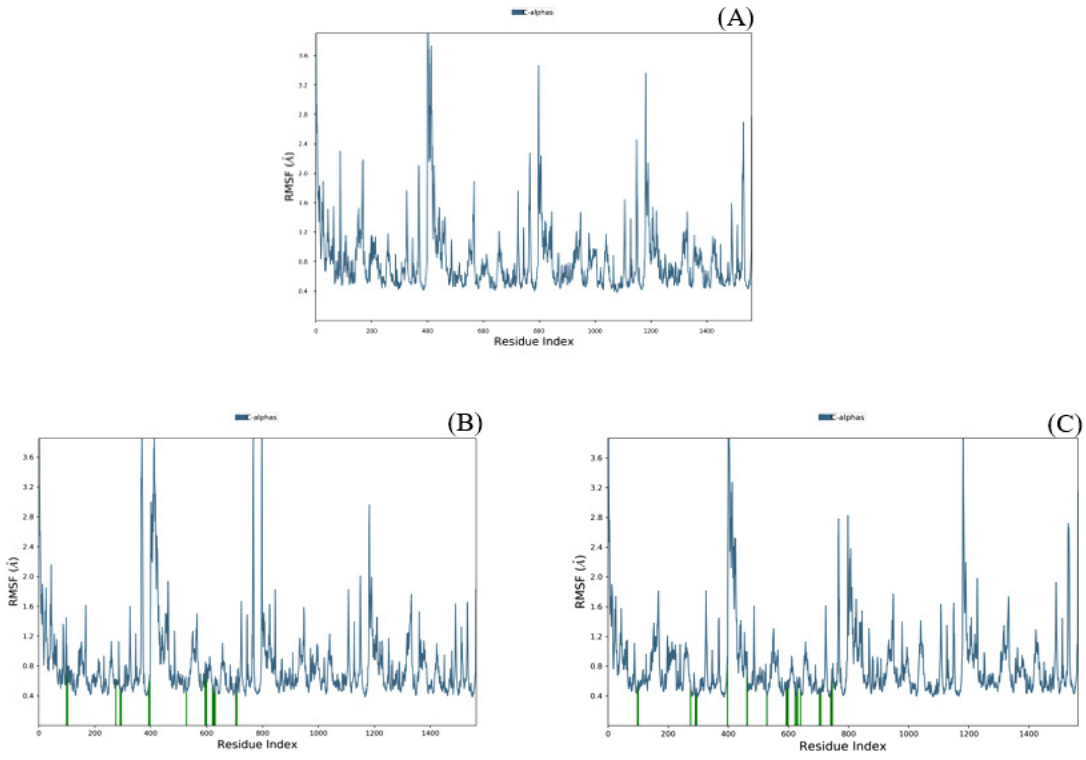

Fig. 4 Root mean square fluctuation (RMSF) plots of: (A) apo protein 1HW9; (B) 1HW9-simvastatin complex; (C) 1HW9–6′-*O*-(3″-hydroxy-3″-methylglutaryl)-6′,7′-dihydroxybergamottin (CH1) complex, where protein residues that interact with ligands are marked with green-colored vertical bars

The protein-ligand interactions obtained after calculation (Fig. 5) were categorized into four types: hydrogen bonds, hydrophobic interaction, ionic interaction and water bridges. The stacked bar charts were obtained after normalization over the course of the trajectory. An interaction fraction value, for example of 0.7 suggests that 70% of the simulation time the specific interaction is maintained. Values over 1.0 may be due to some protein residues making more than one type of interaction with the ligand. Among the four investigated compounds, the residues participating in the substrate hydrogen-bond binding were: LYS 735, ARG 590, LYS 691, ASP 690 and ALA 751 for simvastatin; LYS 735, ARG 590, LYS 691, ASP 690, ASN 658, MET 655, GLY 656, LYS 692 and SER 684 for CH1; ARG 590, LYS 691, ASP 690, ASN 567, ASN 755, GLU 665 and GLU 559 for citrusoside G; and LYS 735 and ALA 525 for for 6′,7′-dihydroxybergamottin (Table 1 and Fig. 6). CH1 and citrusoside G had higher hydrogen-bond interactions than simvastatin, while 6′,7′-dihydroxybergamottin had two hydrogen bond interactions with only one common amino acid residue. Based on the calculations, the presence of a flavonoid moiety, and in particular a 3′′-hydroxy-3′′-methylglutaryl moiety connected to the C10 prenylfuranocoumarin backbone, played a crucial role in bioactivity modulation. However, based on the physicochemical properties (Table 2), CH1 was a better drug candidate. Finally, the molecular docking calculation revealed that a less active compound was 2′-*O*-(3′′-hydroxy-3′′-methylglutaryl)-oxypencedanin hydrate, a compound having a 3′′-hydroxy-3′′-methylglutaryl group attached to the core prenylfuranocoumarin but with a C5 prenyl side chain (Table S1), thus indicating that the chain length of the prenyl group played some role in governing the bioactivity as well.

The analysis is shown in Fig. 6 of the ligand-protein contacts through hydrogen bonding between simvastatin-protein 1HW9 and CH1-protein 1HW9 using MD simulation. Both compounds had stabilized forms in most of the trajectories and the encountered complexes were more consistent with many crucial amino acid residues. CH1 in the CH1-protein 1HW9 complex interacted with ASP-690 (98%), ASN-658 (95%) and ARG-590 (81%) through hydrogen bridges and LYS-735 (51% and 47%, respectively) and with HIS-752 (34%) through water bridges. Simvastatin in the simvastatin-protein 1HW9 complex was consistent with ASN-755 (92%), GLU-559 (82%), SER-684 (38%) and ALA-751 (22%) through hydrogen bridges, while with LYS-735 (41%) and GLU-559 (38%), it was through water bridges.

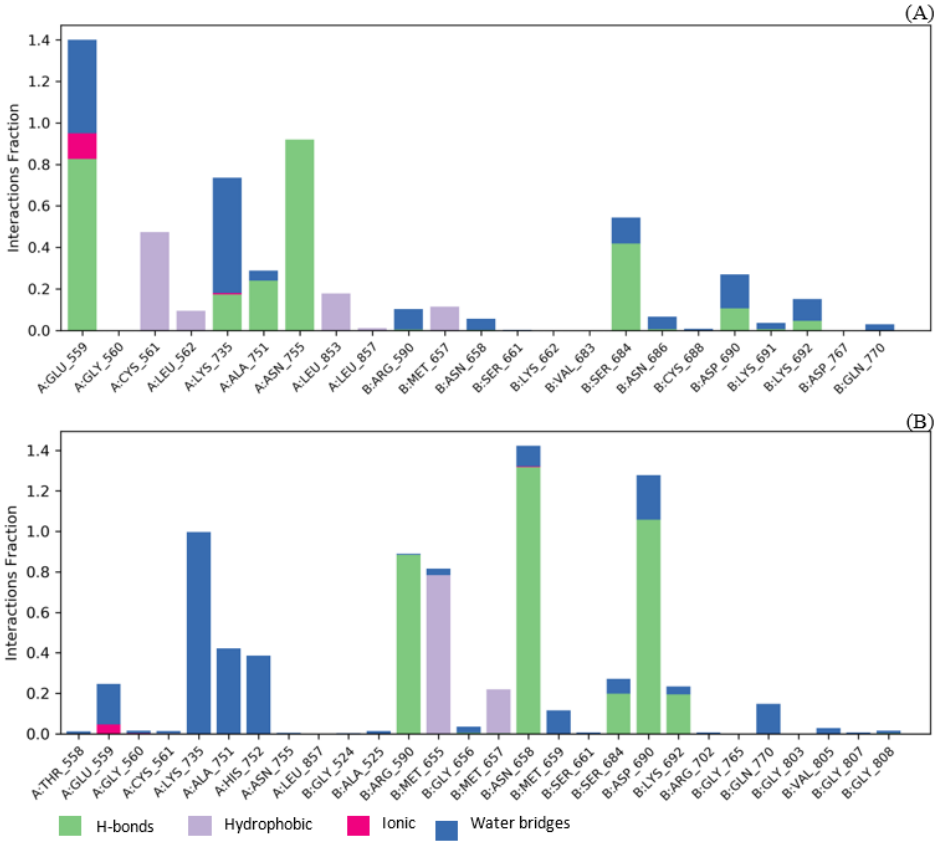

Fig. 5 Protein-ligand interaction fractions of: (A) simvastatin; (B) 6′-*O*-(3′′-hydroxy-3′′-methylglutaryl)-6′,7′-dihydroxybergamottin (CH1)

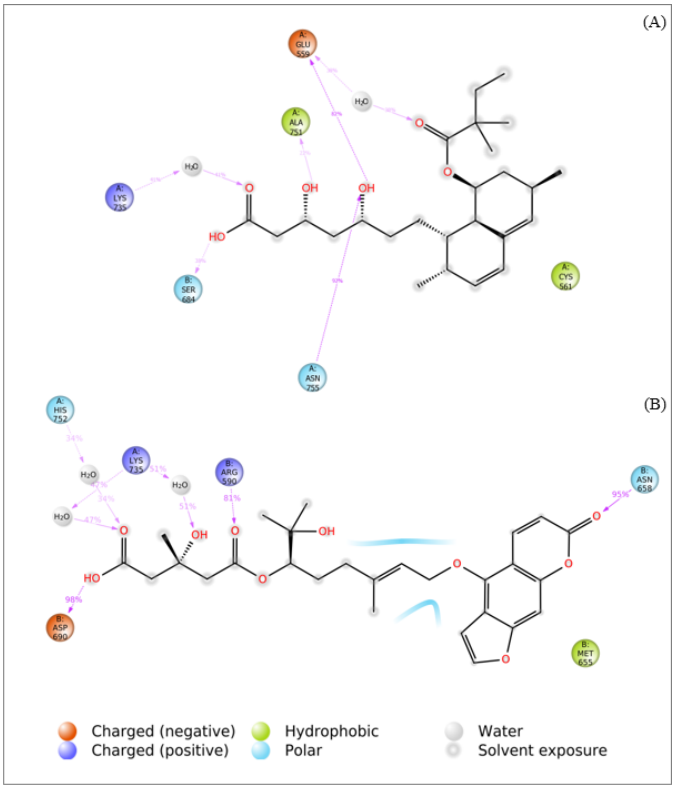

Fig. 6 Ligand-protein contacts based on hydrogen bonding analysis from molecular dynamic simulations of the protein 1HW9 with a ligand: (A) simvastatin; (B) 6′-*O*-(3′′-hydroxy-3′′- methylglutaryl)-6′,7′-dihydroxybergamottin (CH1), where interactions not shown that occurred in less than 22.0% of the simulation time in the selected trajectory (0.00–100.00 ns)

Based on the *in silico* calculations, including molecular docking and MD simulations, CH1 had comparable binding affinity for the HMG-CoA reductase to the standard drug, simvastatin. The MM/GBSA binding interaction of CH1 against the 1HW9 protein was slightly better than for simvastatin. The analysis of the data obtained from the RMSF calculations regarding the protein-ligand and ligand-protein interactions revealed that the different compound structures had different types and numbers of binding interactions.

Results based on three replicates, the *in vitro* HMGCR inhibitory activity assay of the three isolates together with simvastatin was performed using the HMG-CoA reductase assay kit and their IC_{50} values are shown in Table 3. CH1 had the highest inhibitory activity (IC_{50} 114.7 µM) among the three compounds. However, none of the three inhibitory IC_{50} values were as active as simvastatin (IC_{50} 0.72 µM). The discrepancy between the *in vitro* evaluation and *in silico* results may have been due partly to the limited solubility of the hydrophobic compounds in the test buffer solution used.

Notably, another study by the current research team (Youkwan et al., 2010) identified some isolated compounds, in particular, 6′,7′-dihydroxybergamottin, with *in vitro* anticholinesterase activity (Table S3); however, the *in silico* calculation has not yet been carried out. In the current study, additional molecular docking calculations of galanthamine and 6′,7′-dihydroxy bergamottin (one of the most active against an *in vitro* anti-butyrylcholinesterase assay showing an IC_{50} value of 15.4 µM compared to galantamine, with an IC_{50} value of 3.2 µM) were performed against butyrylcholinesterase, BChE (PDB: 4BDS, 2.10 Å) (Cheung et al., 2012). Their binding energy and binding sites are reported in comparison to the standard drug, galantamine (Table S2 and Fig. S1.). An i*n silico* calculation showed that 6′,7′-dihydroxy-bergamottin bound to several key amino acids in the BChE, rather similar to those in galantamine (Fig. S2., Table S2). The current calculation results provided additional data concerning the anti-butyrylcholinesterase activity of 6′,7′-dihydroxybergamottin and thus substantiated

Table 3 *In vitro* HMG-CoA reductase inhibitory activity and *in silico* binding scores of selected isolated compounds

Compound	IC_{50} value (µg/mL)	IC_{50} value (µM)	Activity ratio	HMGCR Docking score	Structure
6′-*O*-(3′′-hydroxy-3′′-methylglutaryl)-6′,7′-dihydroxybergamottin (CH1)	59.1 ± 2.8	114.7	158.9	–9.3	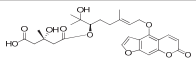
6′,7′-dihydroxy-bergamottin	106.2 ± 1.1	285.4	395.5	–7.6	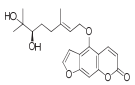
Citrusoside G	252.1 ± 6.4	250.5	347.2	–9.4	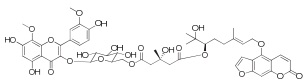
Simvastatin	0.30 ± 0.01	0.72	1.0	–7.4	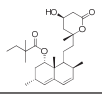

Activity ratio = $IC_{50sample}/IC_{50simvastatin}$; HMGCR = HMG-CoA reductase

the previous proposal that *C. hystrix* constituents may be used to alleviate Alzheimer disease. The current study has provided evidence that the plant may be a useful functional food plant candidate for the treatment and alleviation of hyperglycemia and Alzheimer disease.

Conflict of Interest

The authors declare that they have no known competing financial interests or personal relationships that could have appeared to influence the work reported in this paper.

Acknowledgement

Ramkhamhaeng University provided financial support (FF-2567, Project ID. 201376: 67A112000018). The Center of Excellence for Innovation in Chemistry (PERCH-CIC), Ministry of Higher Education, Science, Research and Innovation provided partial support.

References

Baskaran, G., Salvamani, S., Ahmad, S.A., Shaharuddin, N.A., Pattiram, P.D., Shukor, M.Y. 2015. HMG-CoA reductase inhibitory activity and phytocomponent investigation of *Basella alba* leaf extract as a treatment for hypercholesterolemia. Drug Des. Devel. Ther. 9: 509–517. doi.org/10.2147/DDDT.S75056

BIOVIA, Dassault Systèmes. 2020. BIOVIA Discovery Studio Visualizer version 21.1, San Diego, CA, USA.

Buathong, R., Duangsrisai, S. 2023. Plant ingredients in Thai food: A well-rounded diet for natural bioactive associated with medicinal properties. PeerJ 11: e14568. doi.org/10.7717/peerj.14568

Cheung, J., Rudolph, M.J., Burshteyn, F., Cassidy, M.S., Gary, E.N., Love, J., Franklin, M.C., Height, J.J. 2012. Structures of human acetylcholinesterase in complex with pharmacologically important ligands. J. Med. Chem. 55: 10282–10286. doi.org/10.1021/jm300871x

Dagar, S., Panwar, A., Gahalyan, D., et al. 2025. *In-silico* identification of phytochemicals as potential therapeutic agents to inhibit the HMG-CoA reductase activity using computational approach. Aspect. Mol. Med. 5: 100086. doi.org/10.1016/j.amolm.2025.100086

Daina, A., Michielin, O., Zoete, V. 2017. SwissADME: A free web tool to evaluate pharmacokinetics, drug-likeness and medicinal chemistry friendliness of small molecules. Sci. Rep. 7: 42717. doi.org/10.1038/srep42717

Daina, A., Zoete, V. 2016. A BOILED-egg [*sic*] to predict gastrointestinal absorption and brain penetration of small molecules. Chem. Med. Chem. 11: 1117–1121. doi.org/10.1002/cmdc.201600182

Daina, A., Michielin, O., Zoete, V. 2014. iLOGP: A simple, robust and efficient description of n-octanol/water partition coefficient for drug design using the GB/SA approach. J. Chem. Inf. Model. 54: 3284–3301. doi.org/10.1021/ci500467k

Di Donna, L., De Luca, G., Mazzotti, F., Napoli, A., Salerno, R., Taverna, D., Sindona, G. 2009. Statin-like principles of bergamot fruit (*Citrus bergamia*): Isolation of 3-hydroxymethylglutaryl flavonoid glycosides. J. Nat. Prod. 72: 1352–1354. doi.org/10.1021/np900096w

Frisch, M.J., Trucks, G.W., Schlegel, H.B., et al. 2010. Wallingford CT: Gaussian 09, revision C. 01. https://www.scienceopen.com/document?vid=45b5a7ba-f6ee-40ce-b346-7407f99a540d. 29 September 2025

Gholamhoseinian, A., Shahouzehi, B., Sharifi-Far, F. 2010. Inhibitory activity of some plant methanol extracts on 3-hydroxy-3-methylglutaryl coenzyme A reductase. Int. J. Pharmacol. 6: 705–711. doi.org/10.3923/ijp.2010.705.711

Igel, M., Sudhop, T., Von Bergmann, K. 2001. Metabolism and drug interactions of 3-hydroxy-3-methylglutaryl coenzyme A-reductase inhibitors (statins). Eur. J. Clin. Pharmacol. 57: 357–364. doi.org/10.1007/s002280100329

Iqbal, D., Khan, M.S., Khan, A., Khan, M.S., Ahmad, S., Srivastava, A.K., Bagga, P. 2014. *In Vitro* screening for β-hydroxy-β-methylglutaryl-CoA reductase inhibitory and antioxidant activity of sequentially extracted fractions of *Ficus palmata* Forsk. BioMed. Res. Int. 2014: 762620. doi.org/10.1155/2014/762620

Istvan, E.S., Deisenhofer, J. 2000. The structure of the catalytic portion of human HMG-CoA reductase. Biochim. Biophys. Acta. Mol. Cell Biol. Lipids. 1529: 9–18. doi.org/10.1016/S1388-1981(00)00134-7

Istvan, E.S., Deisenhofer, J. 2001. Structural mechanism for statin Inhibition of HMG-CoA reductase. Science. 292: 1160–1164. doi.org/10.1126/science.1059344

Istvan, E.S., Palnitkar, M., Buchanan, S.K., Deisenhofer, J. 2000. Crystal structure of the catalytic portion of human HMG-CoA reductase: Insights into regulation of activity and catalysis. EMBO J. 19: 819–830. doi.org/10.1093/emboj/19.5.819

Istvan, E. 2003. Statin inhibition of HMG-CoA reductase: A 3-dimensional view. Atheroscler. Suppl. 4: 3–8. doi.org/10.1016/S1567-5688(03)00003-5

Jameson, J.L., Fauci, A.S., Kasper, D.L., Hauser, S.L., Longo, D.L., Loscalzo, J. 2022. Harrison's Principles of Internal Medicine. 21st ed. New York: McGraw-Hill

Junaidin, J., Lestari, D., Kurniawan, M.F., Ikram, N.K.K. 2022. Ligand-based pharmacophore modelling, molecular docking and molecular dynamic studies of HMG-CoA reductase inhibitors. Inform. Med. Unlocked. 32: 101063. doi.org/10.1016/j.imu.2022.101063

Jung, K.A., Song, T.C., Han, D., Kim, I.H., Kim, Y.E., Lee, C.H. 2005. Cardiovascular protective properties of kiwi fruit extracts *in vitro*. Biol. Pharm. Bull. 28: 1782–1785. doi.org/10.1248/bpb.28.1782

Leopoldini, M., Malaj, N., Toscano, M., Sindona, G., Russo, N. 2010. On the inhibitor effects of bergamot juice flavonoids binding to the 3-hydroxy-3-methylglutaryl-CoA reductase (HMGR) enzyme. J. Agric. Food Chem. 58: 10768–10773. doi.org/10.1021/jf102576j

Mazumder, R., Choudhury, D., Sarkar, A., Ghosh, A., Debnath, S., Debnath, B., Ghosh, R. 2024. *In silico* approach for identification of potential tetracyclic triterpenoids from mushroom as HMG-CoA reductase inhibitor. Aspect. Mol. Med. 4: 100053. doi.org/10.1016/j.amolm.2024.100053

Morris, G.M., Huey, R., Lindstrom, W., Sanner, M.F., Belew, R.K., Goodsell, D.S., Olson, A.J. 2009. AutoDock4 and AutoDockTools4: Automated docking with selective receptor flexibility. J. Comput. Chem. 30: 2785–2791. doi.org/10.1002/jcc.21256

Morris, G.M., Goodsell, D.S., Halliday, R.S., Huey, R., Hart, W.E., Belew, R.K., Olson, A.J., 1998. Automated docking using a Lamarckian genetic algorithm and empirical binding free energy function. J. Comput. Chem. 19: 1639–1662. doi.org/10.1002/(SICI)1096-987X(19981115)19:14<1639::AID-JCC10>3.0.CO;2-B

National Heart, Lung and Blood Institute. 2024. Causes and Risk Factors. https://www.nhlbi.nih.gov/health/blood-cholesterol/causes, 29 September 2025

National Health Service, UK. 2022a. What is high cholesterol? https://www.nhs.uk/conditions/high-cholesterol, 29 September 2025

National Health Service, UK. 2022b. Side effects. https://www.nhs.uk/medicines/statins/side-effects, 29 September 2025

Schrödinger, L.L.C. 2021. Schrödinger release 2021-1: Desmond Molecular Dynamics System, DE Shaw Research. New York.

Shehu, A., Kavraki, L.E. 2012 Modeling Structures and Motions of Loops in Protein Molecules. Entropy 14: 252–290. doi.org/10.3390/e14020252

Siti, H.N., Mohamed, S., Kamisah, Y. 2022. Potential therapeutic effects of *Citrus hystrix* DC and its bioactive compounds on metabolic disorders. Pharmaceuticals 15: 167. doi.org/10.3390/ph15020167

Silva, M., Philadelpho, B., Santos, J., et al. 2021. IAF, QGF and QDF peptides exhibit cholesterol-lowering activity through a statin-like HMG-CoA reductase regulation mechanism: *in silico* and i*n vitro* approach. Int. J. Mol. Sci. 22: 11067. doi.org/10.3390/ijms222011067

Seeka, C., Sutthivaiyakit, P., Youkwan, J., Hertkorn, N., Harir, M., Schmitt-Kopplin, P., Sutthivaiyakit, S. 2016. Prenylfuranocoumarin-HMGA-flavonol glucoside conjugates and other constituents of the fruit peels of *Citrus hystrix* and their anticholinesterase activity.Phytochemistry127:38–49.doi.org/10.1016/j.phytochem.2016.03.009

Stein. E.A. 2002. Managing dyslipidemia in the high-risk patient. Amer. J. Cardiol. 89: 50–57. doi.org/10.1016/S0002-9149(02)02229-4

Trott, O., Olson, A.J. 2009. AutoDock Vina: improving the speed and accuracy of docking with a new scoring function, efficient optimization and multithreading. J. Comput. Chem. 31: 455–461. doi.org/10.1002/jcc.21334

Youkwan, J., Sutthivaiyakit, S., Sutthivaiyakit, P. 2010. Citrusosides A–D and furanocoumarins with cholinesterase inhibitory activity from the fruit peels of *Citrus hystrix*. J. Nat. Prod. 73: 1879–1883. doi.org/10.1021/np100531x

Zaborowska, M., Matyszewska, D., Bilewicz, R. 2022. Model lipid raft membranes for embedding integral membrane proteins: reconstitution of HMG-CoA reductase and its inhibition by statins. Langmuir. 38: 13888–13897. doi.org/10.1021/acs.langmuir.2c02115

Zhao, Z., Wang, Y., Nian, M., et al. 2023. *Citrus hystrix*: A review of phytochemistry, pharmacology and industrial applications research progress. Arab. J. Chem. 16: 105236. doi.org/10.1016/j.arabjc.2023.105236